Latin American Journal of Solids and Structures
www.lajss.org

Numerical study of concrete-filled steel composite (CFSC) stub columns with steel stiffeners

Abstract
Numerical study of concrete-filled steel composite (CFSC) stub columns with steel stiffeners is presented in this paper. The behaviour of the columns is examined by the use of the finite element software LUSAS. Results from nonlinear finite element analyses are compared with those from corresponding experimental tests which uncover the reasonable accuracy of the modelling. Novel steel stiffeners are used in the CFSC stub columns of this study. The columns are extensively developed considering three different special arrangements of the steel stiffeners with various number, spacing, and widths of the stiffeners. The main variables are: (1) arrangement of the steel stiffeners (C1, C2, and C3); (2) number of the steel stiffeners (2 and 3); (3) spacing of the steel stiffeners (50 mm and 100 mm); (4) width of the steel stiffeners (50 mm, 75 mm, and 100 mm); (5) steel thickness (2 mm, 2.5 mm, and 3 mm); (6) concrete compressive strength (30 MPa, 40 MPa, and 50.1 MPa); (7) steel yield stress (234.3 MPa, 350 MPa, and 450 MPa). Effects of the variables on the behaviour of the columns are assessed. Failure modes of the columns are also illustrated. It is concluded that the variables have considerable effects on the behaviour of the columns. Moreover, ultimate load capacities of the columns are predicted by the design code EC4, suggested equation of other researchers, and proposed equation of the authors of this paper. The obtained ultimate load capacities from the analyses are compared with the predicted values. It concludes that EC4 gives more conservative predictions than the equations.

Keywords
Numerical study, composite column, steel stiffener, nonlinear finite element analysis, ultimate load capacity, ductility.

Alireza Bahrami*
Wan Hamidon Wan Badaruzzaman
Siti Aminah Osman

Department of Civil and Structural Engineering, Universiti Kebangsaan Malaysia, Bangi, Selangor, Malaysia

* Author email: bahrami_a_r@yahoo.com

1 INTRODUCTION

Greater structural performance accomplished by concrete-filled steel composite (CFSC) stub columns compared with traditional steel and reinforced concrete columns can be attributed to the efficient composite action between the main constituent materials of the CFSC columns, steel and concrete, which results in their advantages such as large load capacity, better ductility, high stiffness, and also saving of construction cost, time, and manpower. To date, several studies have been carried out on the CFSC columns. Wang (1999) conducted eight tests on concrete-filled rectangular hollow steel section columns. Zhao and Grzebieta (2002) performed a series of compression and

bending tests on concrete-filled double skin tubes to evaluate strength and ductility. Thin-walled steel rectangular hollow section columns filled with concrete under long-term sustained loads were analysed by Han and Yang (2003). Tao et al. (2005) tested concrete-filled steel tubular stub columns under axial compression. Nonlinear behaviour of concrete-filled high strength stainless steel stiffened square and rectangular tubes was studied by Ellobody (2007). An experimental study on concrete-filled composite columns was done by Liew and Xiong (2009) to evaluate the effect of pre-load on the axial capacity of the columns. Tokgoz and Dundar (2010) tested steel tubular columns in-filled with plain and steel fibre reinforced concrete. Petrus et al. (2010) assessed effects of tab stiffeners on the bond and compressive strengths of concrete-filled thin walled steel tubes. Muciaccia et al. (2011) carried out an experimental and analytical investigation on concrete-filled tubes with critical lengths between 131 cm to 467 cm. Yang and Han (2011) performed an experimental study on 28 concrete-filled steel tubular stub columns subjected to eccentric partial compression to assess effects of parameters including section type, load eccentricity ratio, and shape of the loading bearing plate. Behaviour of concrete-filled steel composite slender columns was studied by Bahrami et al. (2011) to develop different shapes (V, T, L, Line & Triangular) and number (1 on side & 2 on side) of longitudinal cold-formed stiffeners and to investigate their effects on the behaviour of the columns. However, no research works are available in the literature on the behaviour of the CFSC stub columns with novel steel stiffeners adopted in this study.

The current study investigates concrete-filled steel composite (CFSC) stub columns with steel stiffeners. The accuracy of the modelling is demonstrated by comparing the results of the experimental tests presented by Tao et al. (2005) with those obtained from the proposed finite element modelling. Novel steel stiffeners are utilised in the columns of this study. The columns are numerously developed using three different special arrangements of the steel stiffeners with various number, spacing, and widths of the stiffeners, steel thicknesses, concrete compressive strengths, and steel yield stresses. Different variables are considered including arrangement of the steel stiffeners (C1, C2, and C3), number of the steel stiffeners (2 and 3), spacing of the steel stiffeners (50 mm and 100 mm), width of the steel stiffeners (50 mm, 75 mm, and 100 mm), steel thickness (2 mm, 2.5 mm, and 3 mm), concrete compressive strength (30 MPa, 40 MPa, and 50.1 MPa), and steel yield stress (234.3 MPa, 350 MPa, and 450 MPa). Effects of different arrangements, number, spacing, and widths of the steel stiffeners, and also steel thicknesses on the ultimate load capacity and ductility of the columns are assessed. Effects of various concrete compressive strengths and steel yield stresses on the ultimate load capacity of the columns are examined. Failure modes of the columns are evaluated. The obtained ultimate load capacities of the columns are thereafter compared with the predicted values by the design code EC4 (2004) and proposed equations of previous research works.

2 FINITE ELEMENT MODELLING

Concrete-filled steel composite (CFSC) stub columns which were experimentally tested by Tao et al. (2005) were considered in this paper for the verification of the finite element modelling using the finite element software LUSAS. The cross sections of the columns with the lengths (L) of 750 mm and 390 mm are shown in Figure 1. The steel thickness of the columns was 2.5 mm.

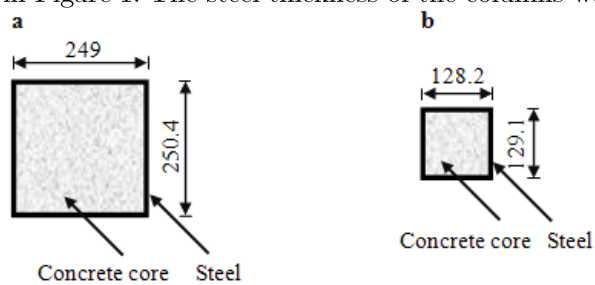

Figure 1: Cross sections of CFSC stub columns: (a) L = 750 mm, (b) L = 390 mm; (dimensions are in mm)

2.1 Material properties and constitutive models

Steel and concrete are the two main materials used in the numerical analysis of the columns which their properties and constitutive models are presented below:

2.1.1 Steel

Modelling of steel was performed as an elastic-perfectly plastic material in both tension and compression. The stress-strain curve used for steel is shown in Figure 2. The yield stress, modulus of elasticity, and Poisson's ratio of steel were respectively as 234.3 MPa, 208,000 MPa, and 0.247 in the corresponding experimental tests of both the columns with the lengths of 750 mm and 390 mm which were also considered in the verification modelling of this study. Von Mises yield criterion, an associated flow rule, and isotropic hardening were used in the nonlinear material model.

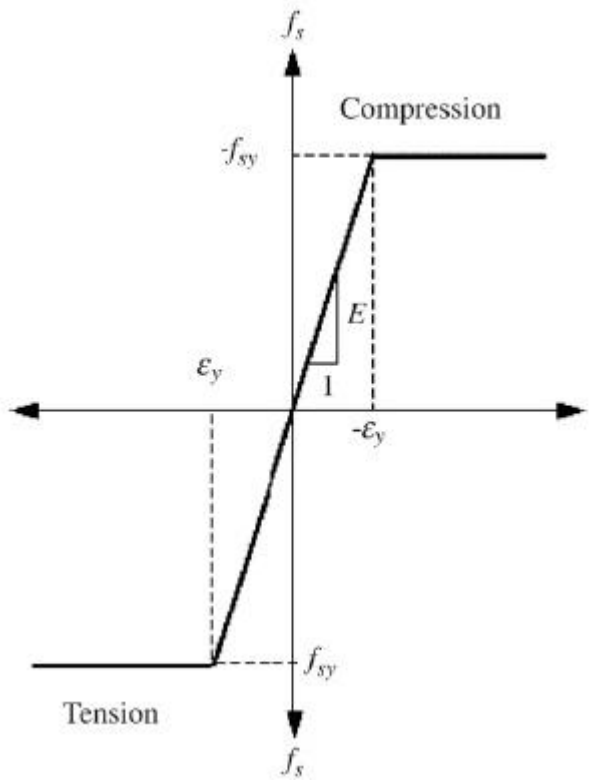

Figure 2: Stress-strain curve for steel

2.1.2 Concrete

The modulus of elasticity of concrete for both the columns with the lengths of 750 mm and 390 mm in the corresponding experimental tests was 35,100 MPa while their concrete compressive strengths were 50.1 MPa and 51.8 MPa, respectively. These material properties of the columns in the experimental tests were exactly taken in the modelling verification too. The equivalent uniaxial stress-strain curves for concrete used by Ellobody and Young (2006a, 2006b) has been also utilised in this study to model concrete, as illustrated in Figure 3. The unconfined concrete cylinder compressive strength f_c is equal to $0.8f_{cu}$ in which f_{cu} is the unconfined concrete cube compressive strength. According to Hu et al. (2005), the corresponding unconfined strain ε_c is usually around the

range of 0.002-0.003. They took ε_c as 0.002. The same value for ε_c has been also considered in the analysis herein. When concrete is under laterally confining pressure, the confined compressive strength f_{cc} and the corresponding confined strain ε_{cc} are much larger than those of unconfined concrete. f_{cc} and ε_{cc} can be respectively obtained by the use of Equations (1) and (2), as recommended by Mander et al. (1988):

$$f_{cc} = f_c + k_1 f_1 \tag{1}$$

$$\varepsilon_{cc} = \varepsilon_c (1 + k_2 \frac{f_1}{f_c}) \tag{2}$$

where f_1 is the lateral confining pressure of steel on the concrete core. The approximate value of f_1 can be determined from the interpolation of the values reported by Hu et al. (2003). The factors of k_1 and k_2 have been respectively taken as 4.1 and 20.5, according to Richart et al. (1928). Since f_1, k_1 and k_2 are known f_{cc} and ε_{cc} can be obtained using Equations (1) and (2).

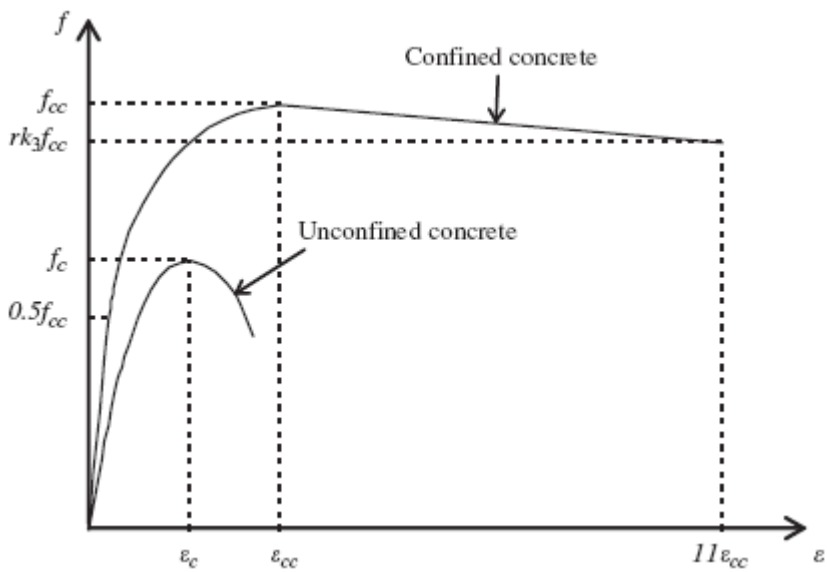

Figure 3: Equivalent uniaxial stress-strain curves for concrete

In accordance with Figure 3, the equivalent uniaxial stress-strain curve for confined concrete includes three parts which are defined. The first part is the initially assumed elastic range to the proportional limit stress. The value of the proportional limit stress has been considered as $0.5f_{cc}$, as given by Hu et al. (2003). The initial Young's modulus of confined concrete E_{cc} has been determined by the use of the empirical Equation (3). The Poisson's ratio v_{cc} of confined concrete has been adopted as 0.2.

$$E_{cc} = 4700\sqrt{f_{cc}} \text{ MPa} \tag{3}$$

The second part is the nonlinear portion which starts from the proportional limit stress $0.5f_{cc}$ to the confined concrete strength f_{cc}. The common Equation (4) presented by Saenz (1964) can be utilised to obtain this part. The values of uniaxial stress f and strain ε are the unknowns of the equation

which define this part of the curve. The strain values ε have been considered between the proportional strain ($0.5f_{cc}/E_{cc}$), and the confined strain ε_{cc} which corresponds to the confined concrete strength. By assuming the strain values ε, the stress values f can be determined using Equation (4).

$$f = \frac{E_{cc}\varepsilon}{1+(R+R_E-2)(\frac{\varepsilon}{\varepsilon_{cc}})-(2R-1)(\frac{\varepsilon}{\varepsilon_{cc}})^2+R(\frac{\varepsilon}{\varepsilon_{cc}})^3} \tag{4}$$

in which R_E and R can be determined from the following equations:

$$R_E = \frac{E_{cc}\varepsilon_{cc}}{f_{cc}}$$

$$R = \frac{R_E(R_\sigma - 1)}{(R_\varepsilon - 1)^2} - \frac{1}{R_\varepsilon}$$

The constants R_ε and R_σ have been considered as 4 in this study, as presented by Hu and Schnobrich (1989). The third part of the curve comprises the descending part that is between f_{cc} and rk_3f_{cc} with the corresponding strain of $11\varepsilon_{cc}$. k_3 is the reduction factor dependent on the H/t ratio. Empirical equations presented by Hu et al. (2003) can be utilised to obtain the approximate value of k_3. The reduction factor r was presented by Ellobody et al. (2006) on the basis of the experimental study done by Giakoumelis and Lam (2004) to consider the effect of different concrete strengths. As Tomii (1991) and also Mursi and Uy (2003) recommended, the value of r has been adopted as 1.0 for concrete with cube strength f_{cu} equal to 30 MPa and as 0.5 for concrete with f_{cu} greater than or equal to 100 MPa. The value of r for concrete cube strength between 30 MPa and 100 MPa has been interpolated in this study.

2.2 Finite element type, concrete-steel interface, boundary conditions, load application, and mesh size

The 6-noded triangular shell element, TSL6, was used for modelling of steel. This is a thin, doubly curved, isoparametric element which can be utilised to model three-dimensional structures. It possesses six degrees of freedom per node and provides accurate solution to most applications. The element formulation takes account of both membrane and flexural deformations. The 10-noded tetrahedral element, TH10, was utilised to model the concrete core. This is a three-dimensional isoparametric solid continuum element capable of modelling curved boundaries. This element is a standard volume element of the LUSAS software (Finite Element Analysis Ltd. 2006).

Slide-lines were utilised to represent the contact between the concrete core and steel (including steel wall and steel stiffeners). The slide-lines are attributes which can be employed to model contact surfaces in the finite element software LUSAS (Finite Element Analysis Ltd. 2006). The slide-line contact facility is nonlinear and was used in the nonlinear analyses. In order to provide the contact between surfaces of steel and concrete, slave and master surfaces needed to be correctly selected. If a smaller surface is in contact with a larger surface, the best selection of the slave surface can be the smaller surface. If this point is impossible to be distinguished, the best selection for the master surface should be the body which possesses higher stiffness. It needs to be clarified that the stiffness of the structure should be considered not the material only. Although, the steel material has higher stiffness than the concrete material, steel in the columns may have less stiffness than the volume of the concrete core in this study. As a consequence, the concrete core and steel surfaces were respectively adopted as the master and slave surfaces. This process of choosing master and slave surfaces has been also reported by Dabaon et al. (2009). The definition of friction coefficient is allowed in the slide-lines. The friction between surfaces of steel and concrete is considered so that

they remain in contact. The Coulomb friction coefficient was chosen as 0.25 in the slide-lines. The slide-lines allow the concrete core and steel to separate or slide but not to penetrate each other.

Pin-ended supports considered in the experimental tests by Tao et al. (2005) have been exactly simulated in the finite element modelling in this study. Thus, the rotations of the top and bottom surfaces of the columns in the X, Y, and Z directions were set to be free. Also, the displacements of the bottom and top surfaces in the X and Z directions were restrained. On the other hand, the displacement of the bottom surface in the Y direction was restrained while that of the top surface, in the direction of the applied load and where the load was applied, was considered to be free.

The axial loading of the experimental tests has been accurately simulated in this study using incremental displacement load with an initial increment of 1 mm applied axially to the top surface of the columns in the negative Y direction.

Different finite element mesh sizes were examined to obtain a reasonable mesh size which can accomplish accurate results. It was finally concluded that the mesh size corresponding to 7713 and 1573 elements respectively for the columns with $L = 750$ mm and $L = 390$ mm can be led to exact results. Figure 4 shows typical finite element meshes of the columns in this study.

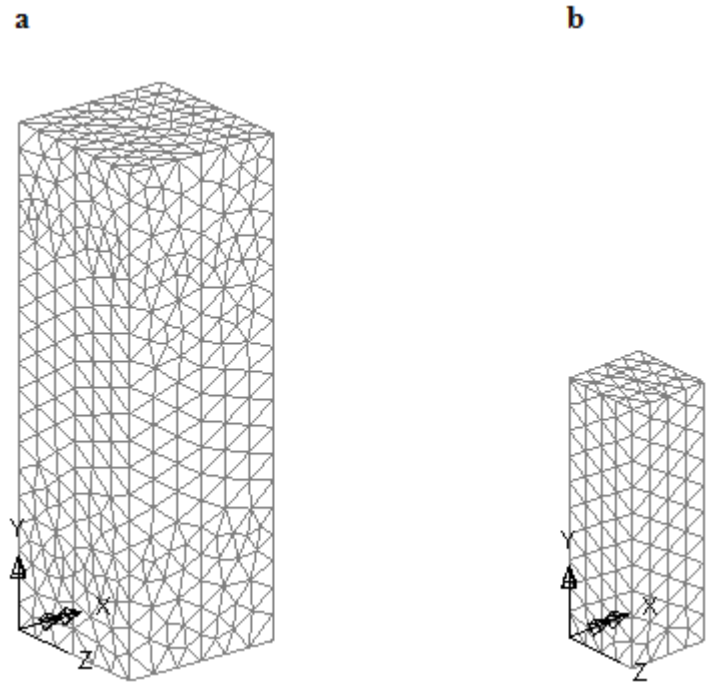

Figure 4: Typical finite element meshes of the columns: (a) L = 750 mm, (b) L = 390 mm

2.3 Modelling accuracy

In order to reveal the accuracy of the finite element modelling in this study, the modelling results were compared with the experimental test results presented by Tao et al. (2005). According to Figure 5, the load-normalised axial shortening curves obtained from the modelling and corresponding experimental tests lie reasonably close to each other, thus establishing the accuracy of the modelling. The obtained ultimate load capacities from the nonlinear finite element analyses of the CFSC stub columns with the lengths of 750 mm and 390 mm are respectively as 3325 kN and 1186 kN while those from the experimental tests of the same columns are respectively as 3230 kN and 1150

kN. The comparison between the ultimate load capacities obtained from the modelling and experimental tests of the columns implies the differences of 2.9% and 3.1% respectively for the columns with the lengths of 750 mm and 390 mm. These small differences show the accuracy of the modelling in this study. Consequently, the proposed finite element modelling can predict the behaviour of the columns with an adequate accuracy herein.

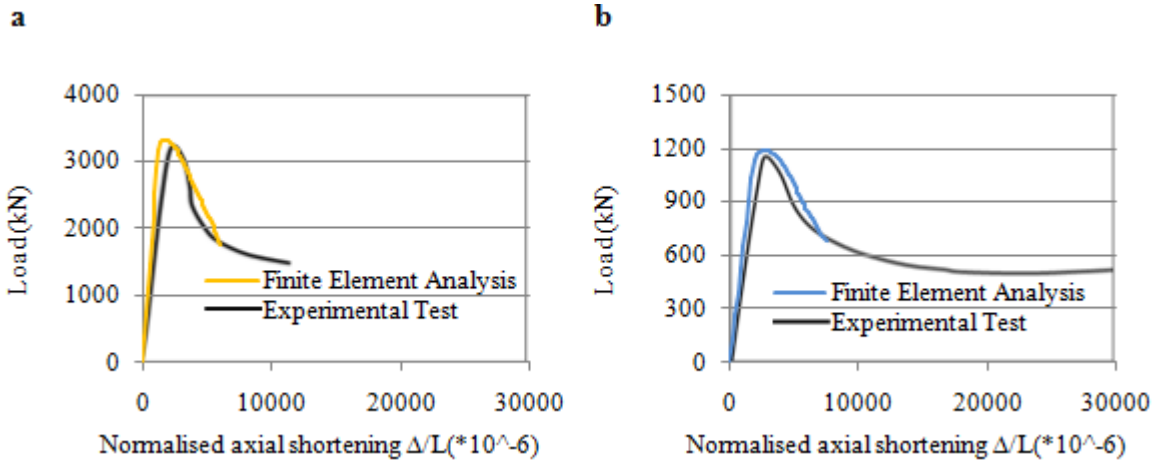

Figure 5: Load versus normalised axial shortening curves for the columns: (a) L = 750 mm, (b) L = 390 mm

3. NUMERICAL ANALYSIS

Because the proposed finite element modelling of this study was uncovered to be sufficiently accurate, the method was utilised for the nonlinear analysis of stub columns of same cross section (B = 249 mm & H = 250.4 mm) and length (L = 750 mm) as that tested by Tao et al. (2005) but with steel stiffeners. Each of the CFSC stub columns was exactly modelled based on the aforementioned modelling specifications. New steel stiffeners were utilised in the current study. Arrangements of the steel stiffeners in the CFSC stub columns are shown in Figure 6 (a, b, & c) which were analysed by the use of nonlinear finite element method. According to the figure, 3 various special arrangements of the steel stiffeners namely C1, C2, and C3 were considered in this study. Also, different number (2 and 3), spacing (50 mm and 100 mm), and widths of the steel stiffeners (50 mm, 75 mm, and 100 mm) were adopted in the analyses in which 4 typical elevations are illustrated in Figure 7 (a, b, c & d). Moreover, Figure 8 shows typical finite element meshes of the stiffened CFSC columns.

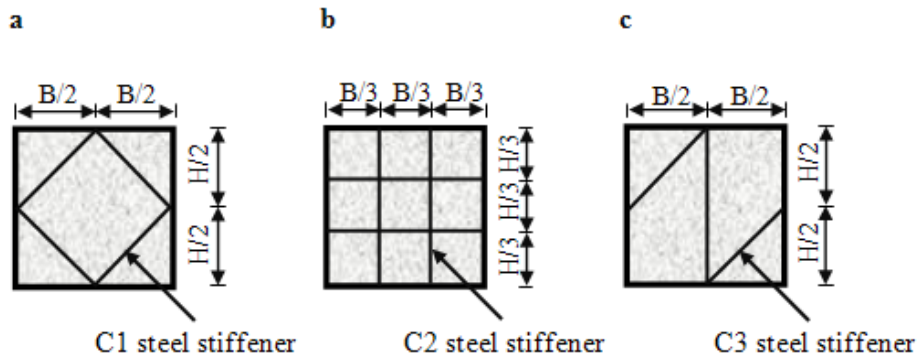

Figure 6: Arrangements of steel stiffeners in CFSC columns: (a) C1 steel stiffener, (b) C2 steel stiffener, (c) C3 steel stiffener

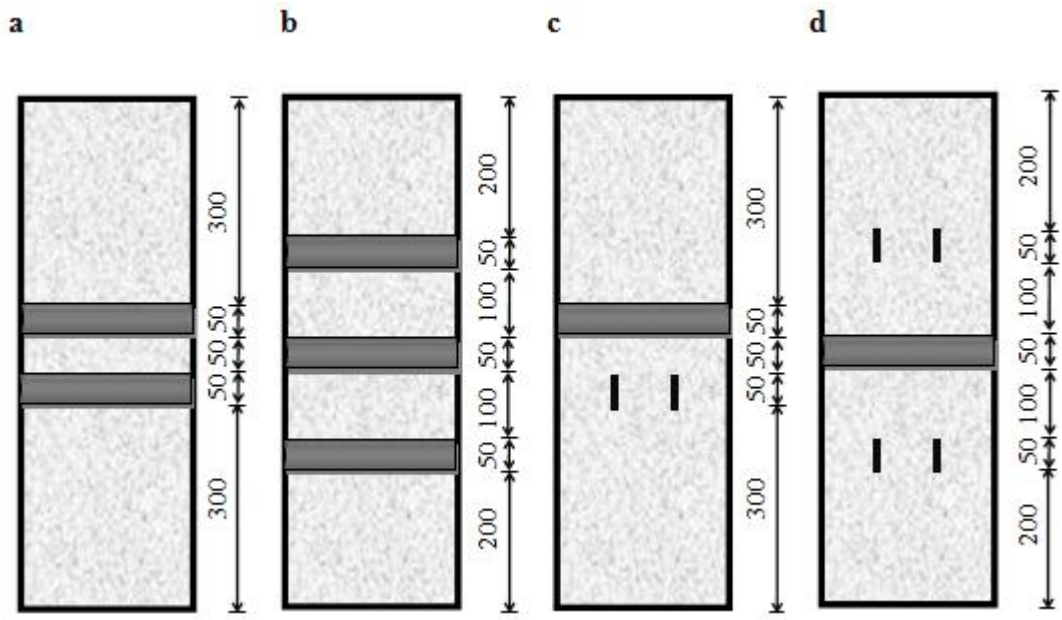

Figure 7: Typical elevations of stiffened CFSC columns (L = 750 mm): (a) columns with C1 or C3 steel stiffeners, 2 stiffeners with width and spacing of 50 mm, (b) columns with C1 or C3 steel stiffeners, 3 stiffeners with width of 50 mm and spacing of 100 mm, (c) columns with C2 steel stiffeners, 2 stiffeners with width and spacing of 50 mm, (d) columns with C2 steel stiffeners, 3 stiffeners with width of 50 mm and spacing of 100 mm; (dimensions are in mm)

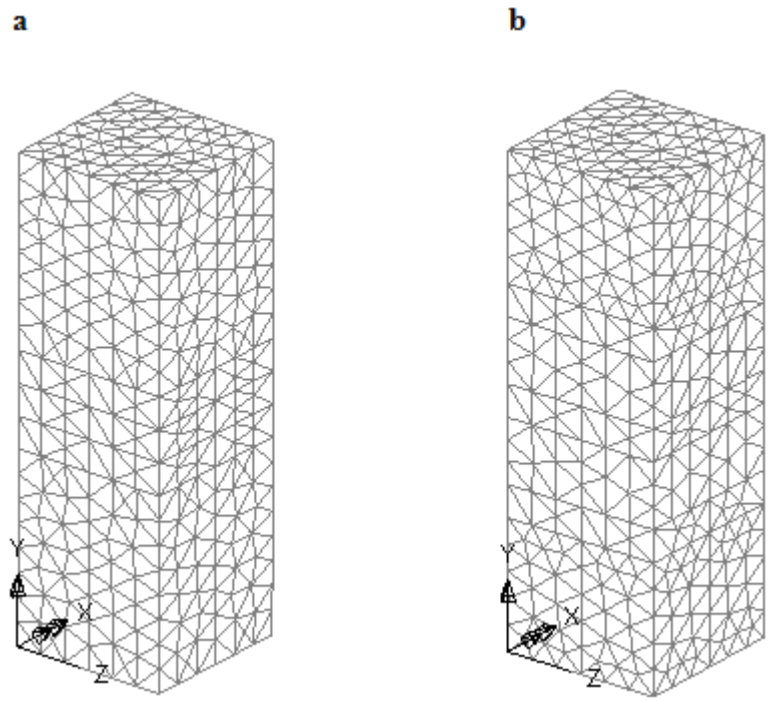

Figure 8: Typical finite element meshes of the stiffened CFSC stub columns (L = 750 mm): (a) column with C1 steel stiffeners, 2 stiffeners with width and spacing of 50 mm, (b) column with C1 steel stiffeners, 3 stiffeners with width of 50 mm and spacing of 100 mm

4. RESULTS AND DISCUSSION

Table 1 summarises features and obtained ultimate load capacities of the analysed CFSC stub columns. Different special arrangements of the steel stiffeners in the columns are represented by C1, C2, and C3 in the columns labels, as were previously demonstrated in Figure 6 (a, b & c). The first four numbers following C1, C2, and C3 respectively designate the steel thickness t (mm), width of the steel stiffeners W_s (mm), steel yield stress f_y (MPa), and concrete compressive strength f_c (MPa). Also, the number before the parentheses in the columns labels is the number of the steel stiffeners and the number in the parentheses represents the spacing (mm) between the steel stiffeners. It needs to be noted that since the unstiffened CFSC column does not have any kinds of the steel stiffeners, the number in the label corresponding to the steel stiffeners is zero. This point can be seen in the label of the unstiffened CFSC column as C0-2.5-0-234-50-0. Effects of various parameters on the behaviour of the columns are also presented in the sections below.

No.	Column label	t (mm)	W_s (mm)	f_y (MPa)	f_c (MPa)	N_u (kN)
1	C0-2.5-0-234-50-0	2.5	0	234.3	50.1	3325
2	C1-2.5-50-234-50-3(50)	2.5	50	234.3	50.1	3920
3	C1-2.5-50-234-50-2(50)	2.5	50	234.3	50.1	3661
4	C1-2.5-50-234-50-3(100)	2.5	50	234.3	50.1	3734
5	C1-2.5-50-234-50-2(100)	2.5	50	234.3	50.1	3566
6	C2-2.5-50-234-50-3(50)	2.5	50	234.3	50.1	3783
7	C2-2.5-50-234-50-2(50)	2.5	50	234.3	50.1	3570
8	C2-2.5-50-234-50-3(100)	2.5	50	234.3	50.1	3621
9	C2-2.5-50-234-50-2(100)	2.5	50	234.3	50.1	3486
10	C3-2.5-50-234-50-3(50)	2.5	50	234.3	50.1	3838
11	C3-2.5-50-234-50-2(50)	2.5	50	234.3	50.1	3599
12	C3-2.5-50-234-50-3(100)	2.5	50	234.3	50.1	3663
13	C3-2.5-50-234-50-2(100)	2.5	50	234.3	50.1	3514
14	C1-3-50-234-50-3(50)	3	50	234.3	50.1	4117
15	C1-2-50-234-50-3(50)	2	50	234.3	50.1	3726
16	C1-3-50-234-50-3(100)	3	50	234.3	50.1	3930
17	C1-2-50-234-50-3(100)	2	50	234.3	50.1	3545
18	C1-2.5-100-234-50-3(50)	2.5	100	234.3	50.1	4280
19	C1-2.5-75-234-50-3(50)	2.5	75	234.3	50.1	4114
20	C1-2.5-100-234-50-3(100)	2.5	100	234.3	50.1	4040
21	C1-2.5-75-234-50-3(100)	2.5	75	234.3	50.1	3903
22	C1-2.5-50-234-40-3(50)	2.5	50	234.3	40	3313
23	C1-2.5-50-234-30-3(50)	2.5	50	234.3	30	2702
24	C1-2.5-50-234-40-3(100)	2.5	50	234.3	40	3158
25	C1-2.5-50-234-30-3(100)	2.5	50	234.3	30	2565
26	C1-2.5-50-450-50-3(50)	2.5	50	450	50.1	4719
27	C1-2.5-50-350-50-3(50)	2.5	50	350	50.1	4359
28	C1-2.5-50-450-50-3(100)	2.5	50	450	50.1	4463
29	C1-2.5-50-350-50-3(100)	2.5	50	350	50.1	4155

Table 1: Features and ultimate load capacities (N_u) of the columns

4.1 Effects of arrangement and number of steel stiffeners on ultimate load capacity

As shown in Figures 6 and 7, three various special arrangements of the steel stiffeners (C1, C2, and C3) and different number of the steel stiffeners (2 and 3) were considered in the analyses of CFSC stub columns to investigate their effects on the behaviour of the columns. Figure 9 illustrates these effects on the ultimate load capacity and Table 1 summarises the corresponding ultimate load capacity values of the curves. In accordance with the figure and table, the ultimate load capacity of the unstiffened CFSC stub column (C0-2.5-0-234-50-0) is increased by the use of the steel stiffeners. For example, the ultimate load capacity of the unstiffened column (C0-2.5-0-234-50-0) is 3325 kN which enhances to 3920 kN, 3783 kN, and 3838 kN respectively by the use of 3C1 steel stiffeners (C1-2.5-50-234-50-3(50)), 3C2 steel stiffeners (C2-2.5-50-234-50-3(50)), and 3C3 steel stiffeners (C3-2.5-50-234-50-3(50)) which show the enhancements of 17.9%, 13.8%, and 15.4%, respectively. As a consequence, the hierarchy of different arrangements of the steel stiffeners with the same steel thickness and same number and spacing of the steel stiffeners from the ultimate load capacity view is C1, C3, and C2.

In addition, if the number of the steel stiffeners is enhanced, the ultimate load capacity is increased. For instance, as the number of the steel stiffeners is increased from 2 (C1-2.5-50-234-50-2(50)) to 3 (C1-2.5-50-234-50-3(50)) for the same steel stiffeners spacing of 50 mm, the ultimate load capacity is improved from 3661 kN to 3920 kN, an improvement of 7.1%.

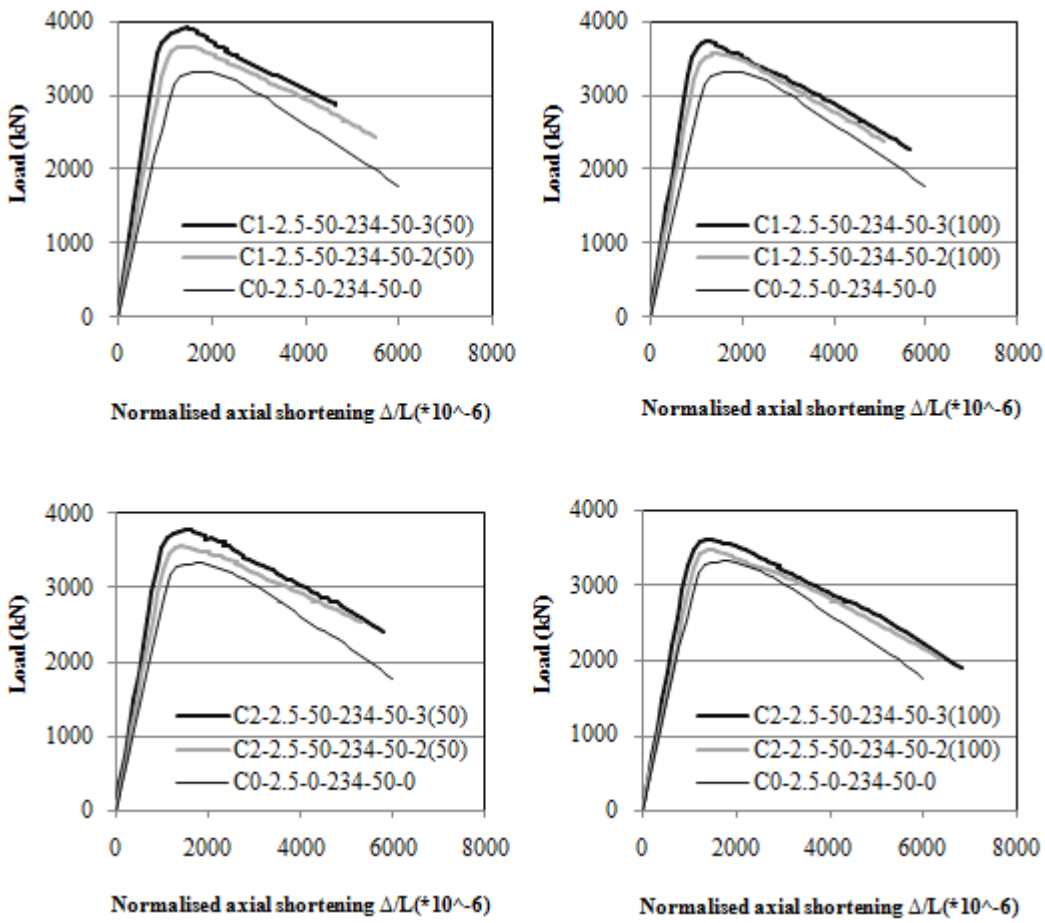

Figure 9: Effects of arrangement and number of steel stiffeners on ultimate load capacity

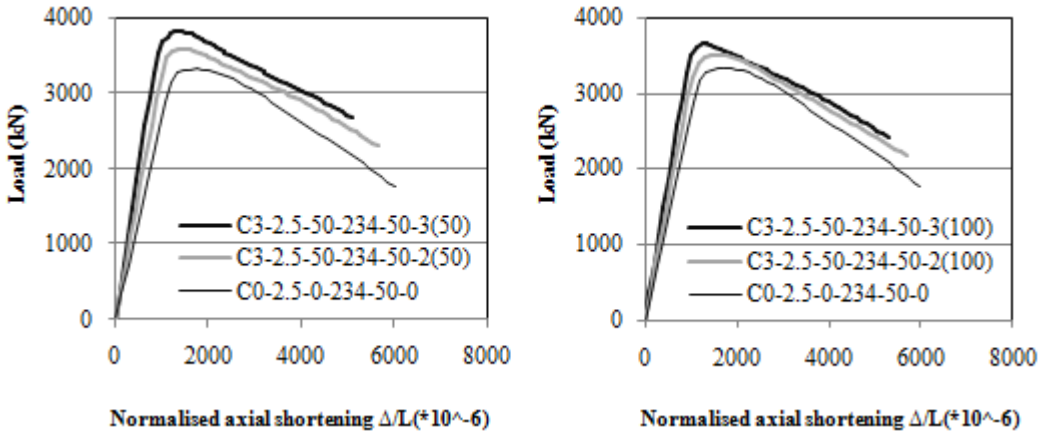

Figure 9: Continued

4.2 Effect of spacing of steel stiffeners on ultimate load capacity

The effect of spacing of steel stiffeners on the behaviour of the CFSC stub columns is investigated by considering two different steel stiffeners spacing of 50 mm and 100 mm in the analyses of the columns with C1, C2, and C3 steel stiffeners. This effect on the ultimate load capacity of the columns is indicated in Figure 10. According the figure and Table 1, the decrease of the steel stiffeners spacing increases the ultimate load capacity. As an example, the ultimate load capacity of the column with the same number of C3 steel stiffeners improves from 3663 kN (C3-2.5-50-234-50-3(100)) to 3838 kN (C3-2.5-50-234-50-3(50)) respectively for the steel stiffeners spacing of 100 mm and 50 mm, an increase of 4.8%.

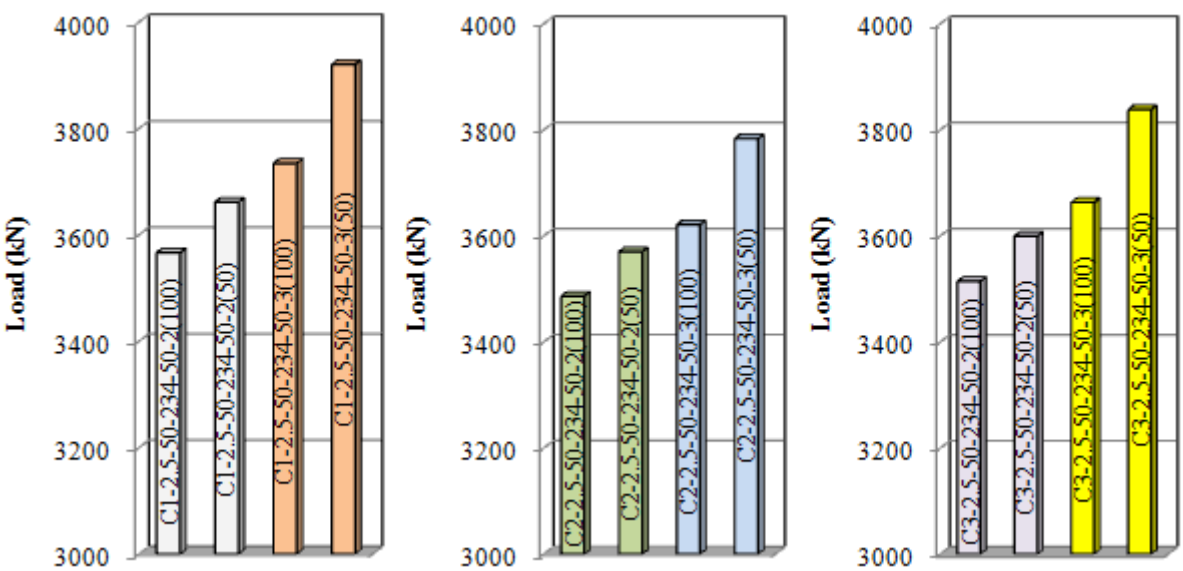

Figure 10: Effect of spacing of steel stiffeners on ultimate load capacity

4.3 Effect of steel thickness on ultimate load capacity

Three various steel thicknesses of 2 mm, 2.5 mm, and 3 mm were considered in the analysed CFSC stub columns with 3C1 steel stiffeners to examine the effect of the steel thickness on the behaviour of the columns. Figure 11 illustrates the results. The steel thickness increase results in the enhancement of the ultimate load capacity (Figure 11 & Table 1). For instance, if the steel thickness enhances from 2 mm (C1-2-50-234-50-3(100)) to 3 mm (C1-3-50-234-50-3(100)) with the same number and spacing of the steel stiffeners, the ultimate load capacity of the column is increased from 3545 kN to 3930 kN, an enhancement of 10.9%.

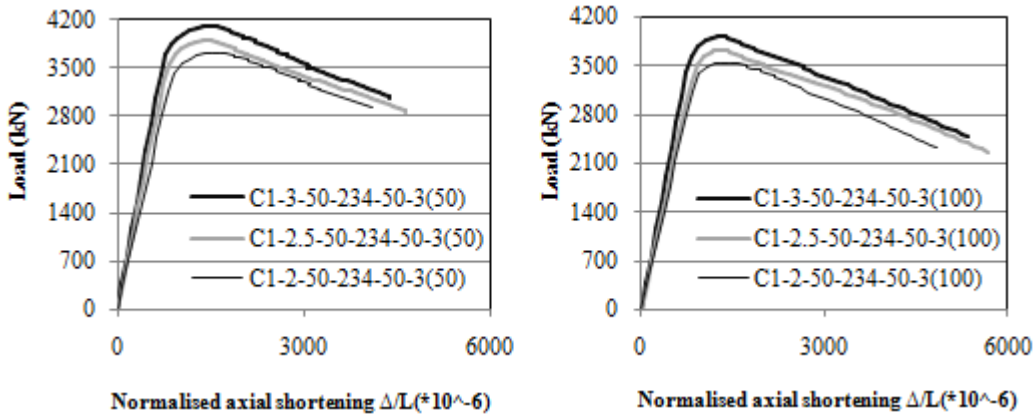

Figure 11: Effect of steel thickness on ultimate load capacity

4.4 Effect of width of steel stiffeners on ultimate load capacity

To assess the effect of width of steel stiffeners on the ultimate load capacity of the CFSC stub columns, three different widths of the steel stiffeners (50 mm, 75 mm, and 100 mm) were used in the analyses of the columns with 3C1 steel stiffeners. According to the obtained results in Figure 12 and its corresponding values in Table 1, larger width of the steel stiffeners leads to higher ultimate load capacity. For instance, enhancing the width of the steel stiffeners from 50 mm (C1-2.5-50-234-50-3(50)) to 100 mm (C1-2.5-100-234-50-3(50)) with the same number and spacing of the steel stiffeners improves the ultimate load capacity from 3920 kN to 4280 kN, an increase of 9.2%.

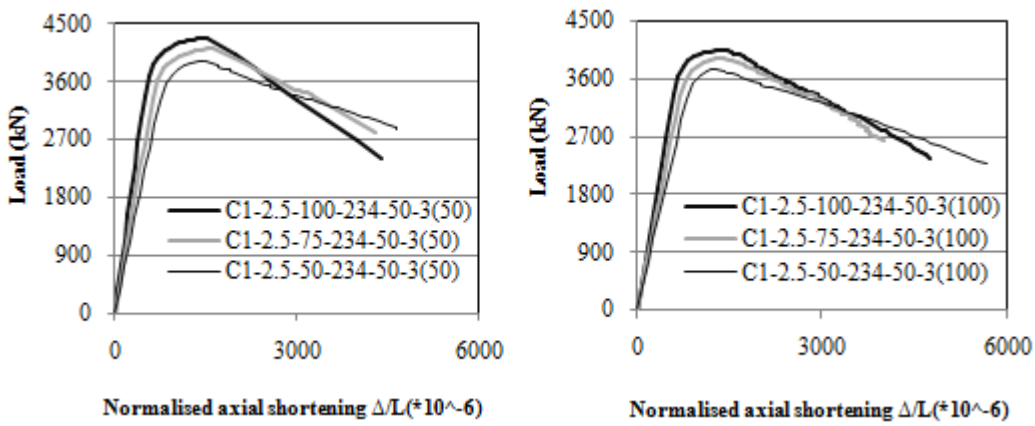

Figure 12: Effect of width of steel stiffeners on ultimate load capacity

4.5 Effects of arrangement, number, and spacing of steel stiffeners on ductility

In order to evaluate the ductility of the columns, a ductility index (DI) defined by Lin and Tsai (2001) has been utilised in this paper. Equation (5) expresses the ductility index:

$$DI = \frac{\varepsilon_{85\%}}{\varepsilon_y} \tag{5}$$

in which $\varepsilon_{85\%}$ is the nominal axial shortening (Δ/L) corresponding to the load which falls to its 85% of the ultimate load capacity and ε_y is $\varepsilon_{75\%}/0.75$ in which $\varepsilon_{75\%}$ is the nominal axial shortening corresponding to the load that obtains 75% of the ultimate load capacity. The values of $\varepsilon_{85\%}$ and ε_y can be taken from Figure 9. Figure 13 illustrates effects of arrangement, number, and spacing of the steel stiffeners on the ductility.

According to Figure 13, the use of the steel stiffeners improves the ductility of the columns. The ductility of the unstiffened column (C0-2.5-0-234-50-0) which can be obtained as 2.85 from Figure 5a and using Equation (5) increases to 3.578, 3.385, and 3.484 (Figure 13) as the maximum ductility achieved respectively utilising 3C1 steel stiffeners (C1-2.5-50-234-50-3(50)), 3C2 steel stiffeners (C2-2.5-50-234-50-3(50)), and 3C3 steel stiffeners (C3-2.5-50-234-50-3(50)) which denote enhancements of 25.5%, 18.8%, and 22.2%, respectively. Therefore, the hierarchy of different arrangements of the steel stiffeners with the same steel thickness and same number and spacing of the steel stiffeners from the ductility view is C1, C3, and C2 which is the same hierarchy as that from the ultimate load capacity view, as discussed in section 4.1.

As can be seen from Figure 13, increasing the number of the steel stiffeners enhances the ductility of the columns. As an example, the ductility of the column (C3-2.5-50-234-50-2(50)) is 3.271 which is enhanced to 3.484 (C3-2.5-50-234-50-3(50)) respectively for 2 and 3 number of the steel stiffeners, an improvement of 6.5%.

Moreover, reducing the steel stiffeners spacing increases the ductility of the columns (Figure 13). For example, by the reduction of the steel stiffeners spacing from 100 mm (C1-2.5-50-234-50-3(100)) to 50 mm (C1-2.5-50-234-50-3(50)) for the same number of the steel stiffeners, the ductility enhances from 3.389 to 3.578, an enhancement of 5.6%.

4.6 Effect of steel thickness on ductility

The effect of steel thickness on the ductility of the columns is also examined by the use of Equation (5). The values of $\varepsilon_{85\%}$ and ε_y in Equation (5) can be determined from Figure 11. This effect on the ductility of the columns is shown in Figure 14. The increase of the steel thickness improves the ductility (Figure 14). For instance, enhancing the steel thickness from 2 mm (C1-2-50-234-50-3(100)) to 3 mm (C1-3-50-234-50-3(100)) increases the ductility of the columns from 3.241 to 3.593, an increase of 10.9%.

4.7 Effect of width of steel stiffeners on ductility

Equation (5) is also used to assess the effect of width of the steel stiffeners on the ductility of the columns. The values of $\varepsilon_{85\%}$ and ε_y in Equation (5) can be obtained from Figure 12. This effect on the ductility of the columns can be observed from Figure 15. It can be noticed from the figure that as a wider steel stiffener is used the ductility of the columns is enhanced. As an example, the enhancement of the steel stiffeners width from 50 mm (C1-2.5-50-234-50-3(50)) to 100 mm (C1-2.5-100-234-50-3(50)) enhances the ductility of the columns from 3.578 to 4.047, an improvement of 13.1%.

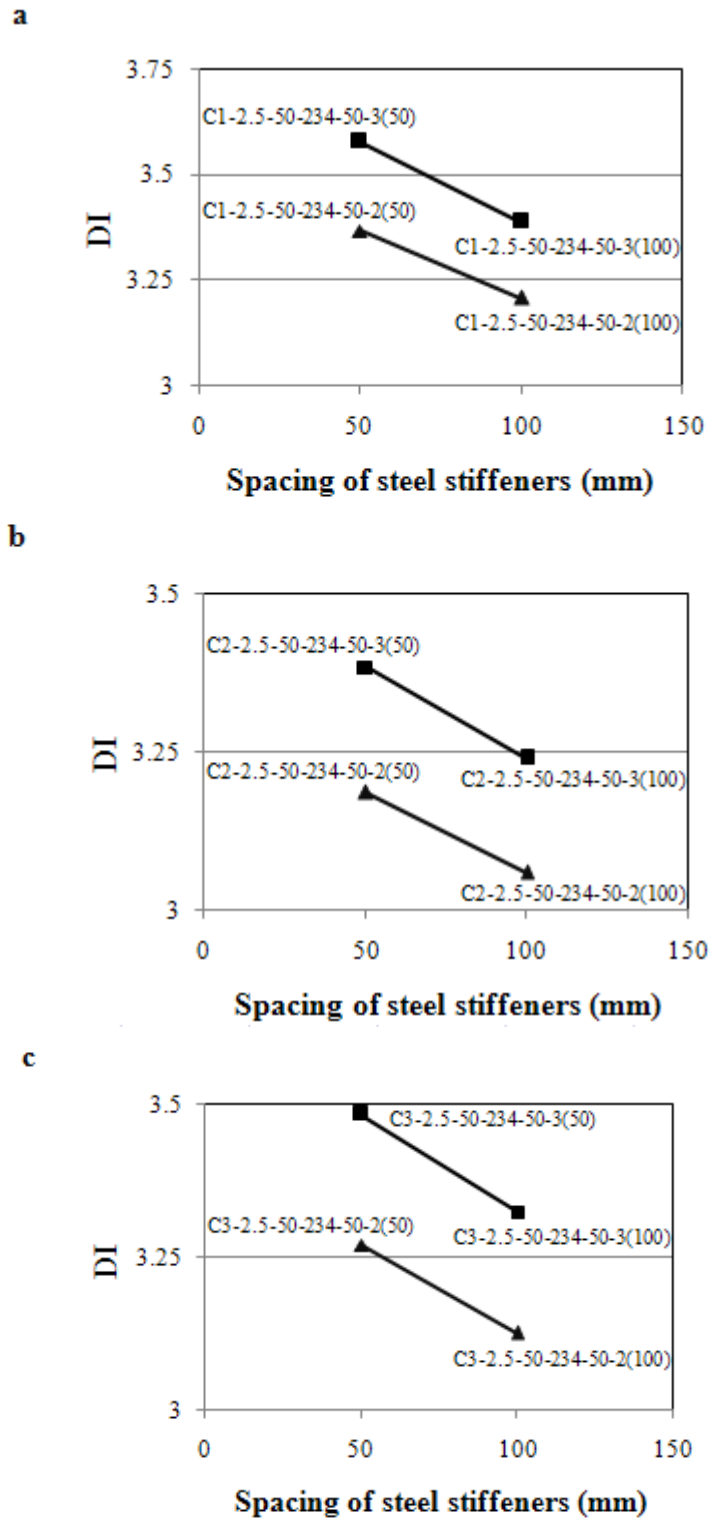

Figure 13: Effects of arrangement, number, and spacing of steel stiffeners on ductility: (a) C1 steel stiffeners, (b) C2 steel stiffeners, (c) C3 steel stiffeners

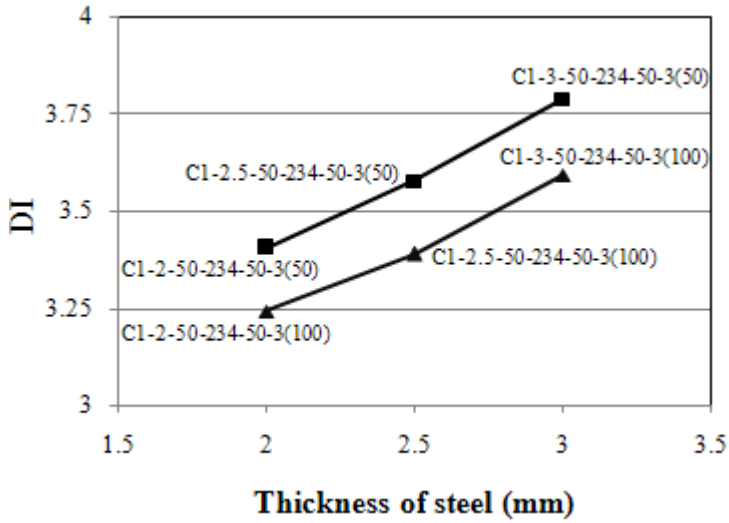

Figure 14: Effect of steel thickness on ductility

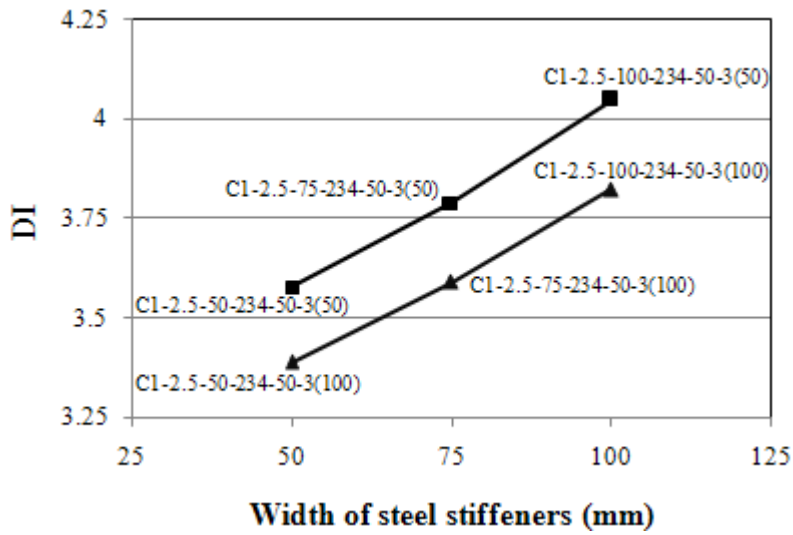

Figure 15: Effect of width of steel stiffeners on ductility

4.8 Effect of concrete compressive strength on ultimate load capacity

Various concrete compressive strengths of 30 MPa, 40 MPa, and 50.1 MPa were adopted in the nonlinear analyses of the columns with 3C1 steel stiffeners to investigate their effects on the ultimate load capacity of the columns. It is obvious from Figure 16 and their corresponding values in Table 1 that the higher concrete compressive strength results in higher ultimate load capacity of the columns. For example, the increase of the concrete compressive strength from 30 MPa (C1-2.5-50-234-30-3(50)) to 50.1 MPa (C1-2.5-50-234-50-3(50)) enhances the ultimate load capacity of the columns from 2702 kN to 3920 kN, an enhancement of 45.1%.

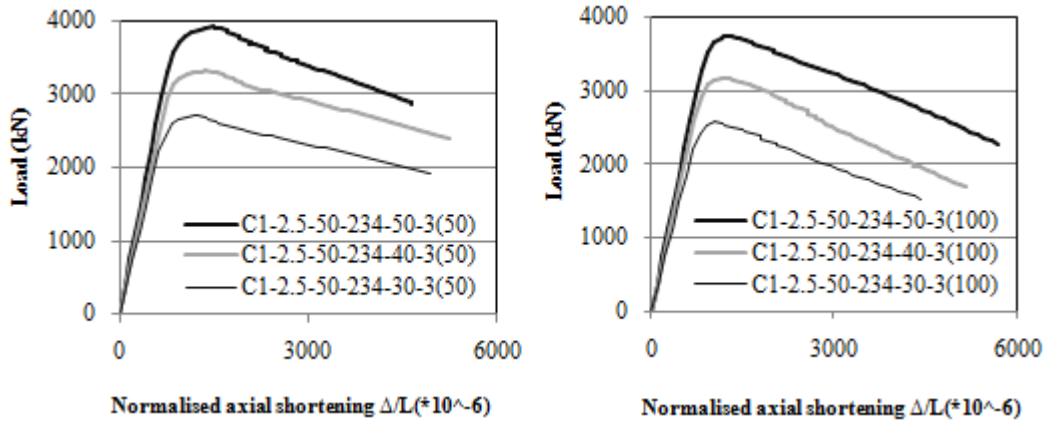

Figure 16: Effect of concrete compressive strength on ultimate load capacity

4.9 Effect of steel yield stress on ultimate load capacity

To assess the effect of steel yield stress on the behaviour of the columns, different steel yield stresses of 234.3 MPa, 350 MPa, and 450 MPa were considered in the analyses of the columns with 3C1 steel stiffeners. This effect is illustrated in Figure 17 along with its corresponding values in Table 1. As the steel yield stress is increased the ultimate load capacity is improved. For instance, by the enhancement of the steel yield stress from 234.3 MPa (C1-2.5-50-234-50-3(100)) to 450 MPa (C1-2.5-50-450-50-3(100)) the ultimate load capacity of the columns enhances from 3734 kN to 4463 kN, an increase of 19.5%.

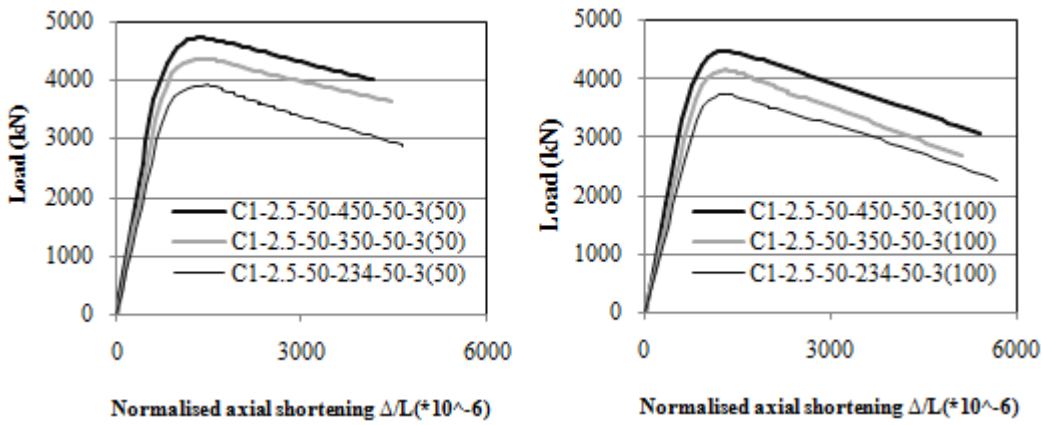

Figure 17: Effects of steel yield stress on ultimate load capacity

4.10 Failure modes

Typical failure modes of the stiffened CFSC stub columns are shown in Figures 18, 19, and 20. As it is obvious from the figures, the failure modes of the columns were characterised by crushing of the concrete core about their mid-height where the local buckling of the steel wall occurred. The infilled concrete prevented the steel wall from the buckling inward.

As stated earlier, the use of the steel stiffeners, enhancement of number or width of the steel stiffeners, reduction of the steel stiffeners spacing, or increase of the steel thickness lead to the im-

provement of the ultimate load capacity and ductility. This improvement can be because of the increased confinement effect of steel on the concrete core due to each of the above-mentioned changes of the parameters. This increased confinement effect delays the local buckling of the steel wall which finally results in the enhancement of the ultimate load capacity and ductility.

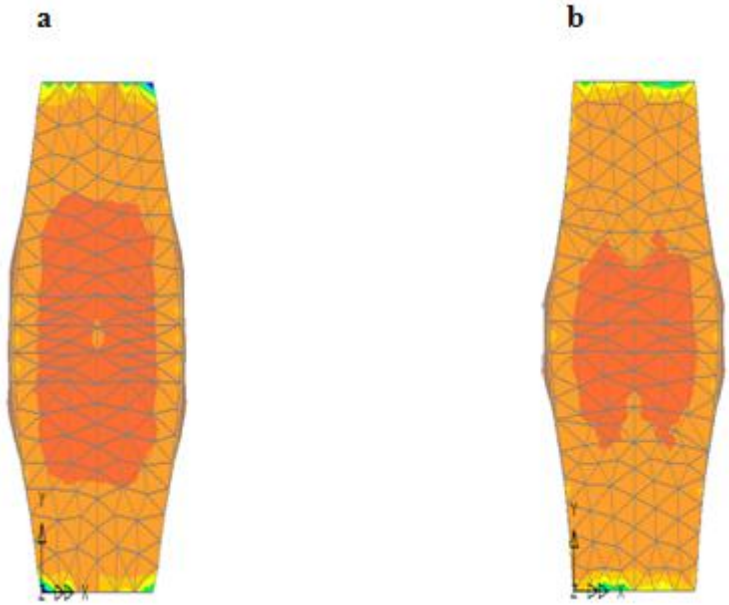

Figure 18: Typical finite element deformed meshes of the stiffened CFSC stub columns: (a) C1-2.5-50-234-50-2(50), (b) C1-2.5-50-234-50-3(100)

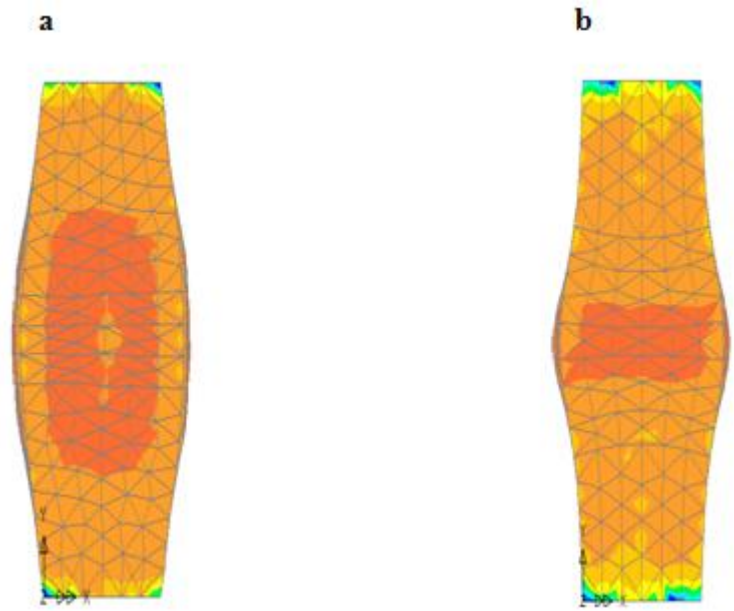

Figure 19: Typical finite element deformed meshes of the stiffened CFSC stub columns: (a) C2-2.5-50-234-50-2(50), (b) C2-2.5-50-234-50-3(100)

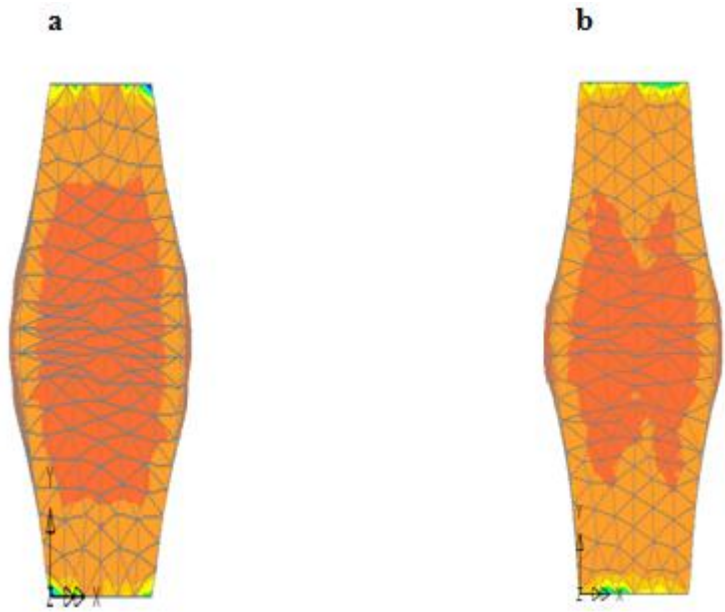

Figure 20: Typical finite element deformed meshes of the stiffened CFSC stub columns: (a) C3-2.5-50-234-50-2(50), (b) C3-2.5-50-234-50-3(100)

4.11 Predictions and comparisons of ultimate load capacity

In accordance with EC4 (2004), Equation (6) can be used to predict the ultimate load capacity of a square or rectangular CFSC stub column:

$$N_{pl,Rd} = A_a f_{yd} + A_c f_{cd} \tag{6}$$

in which A_a and A_c are cross-sectional areas of steel and concrete respectively, and also f_{yd} and f_{cd} are steel yield stress and concrete compressive strength, respectively.

Also, Baig et al. (2006) and Bahrami et al. (2013) proposed Equations (7) and (8) respectively to determine the ultimate load capacity of the columns:

$$P_u = 1.10 A_c f_c + A_a f_y \tag{7}$$

$$N_B = A_a f_{yd} + 1.05 A_c f_{cd} \tag{8}$$

f_c and f_y in Equation (7) are concrete compressive strength and steel yield stress, respectively.

Predicted ultimate load capacities using the above-mentioned equations are compared with the obtained results from the nonlinear analyses of the columns (N_u) in Table 2. SD and COV in Table 2 represent the standard deviation and coefficient of variation, respectively. A mean ratio ($N_{pl,Rd}/N_u$) of 0.897 is obtained with a COV of 0.052 which implies that EC4 (2004) underestimates the ultimate load capacity of the columns by 10.3%. Also, a mean of 0.975 is achieved for P_u/N_u with a COV of 0.056 which shows that Equation (7) gives the ultimate load capacity of the columns by 2.5% lower than those from the nonlinear analyses. In addition, a mean ratio (N_B/N_u) of 0.938 is obtained with a COV of 0.055 which reveals that Equation (8) underestimates the ultimate load capacity by 6.2%. As a result, EC4 (2004) gives more conservative results when compared with those of the proposed Equations (7) and (8).

No.	Column label	N_u (kN)	$N_{pl,Rd}$ (kN)	$N_{pl,Rd}/N_u$	P_u (kN)	P_u/N_u	N_B (kN)	N_B/N_u
1	C1-2.5-50-234-50-3(50)	3920	3409	0.870	3728	0.951	3584	0.914
2	C1-2.5-50-234-50-2(50)	3661	3409	0.931	3728	1.018	3584	0.979
3	C1-2.5-50-234-50-3(100)	3734	3409	0.913	3728	0.998	3584	0.960
4	C1-2.5-50-234-50-2(100)	3566	3409	0.956	3728	1.045	3584	1.005
5	C2-2.5-50-234-50-3(50)	3783	3409	0.901	3728	0.985	3584	0.947
6	C2-2.5-50-234-50-2(50)	3570	3409	0.955	3728	1.044	3584	1.004
7	C2-2.5-50-234-50-3(100)	3621	3409	0.941	3728	1.030	3584	0.990
8	C2-2.5-50-234-50-2(100)	3486	3409	0.978	3728	1.069	3584	1.028
9	C3-2.5-50-234-50-3(50)	3838	3409	0.888	3728	0.971	3584	0.934
10	C3-2.5-50-234-50-2(50)	3599	3409	0.947	3728	1.036	3584	0.996
11	C3-2.5-50-234-50-3(100)	3663	3409	0.931	3728	1.018	3584	0.978
12	C3-2.5-50-234-50-2(100)	3514	3409	0.970	3728	1.061	3584	1.020
13	C1-3-50-234-50-3(50)	4117	3499	0.850	3782	0.919	3641	0.884
14	C1-2-50-234-50-3(50)	3726	3380	0.907	3672	0.986	3526	0.946
15	C1-3-50-234-50-3(100)	3930	3499	0.890	3782	0.962	3641	0.926
16	C1-2-50-234-50-3(100)	3545	3380	0.953	3672	1.036	3526	0.995
17	C1-2.5-100-234-50-3(50)	4280	3409	0.796	3728	0.871	3584	0.837
18	C1-2.5-75-234-50-3(50)	4114	3409	0.829	3728	0.906	3584	0.871
19	C1-2.5-100-234-50-3(100)	4040	3409	0.844	3728	0.923	3584	0.887
20	C1-2.5-75-234-50-3(100)	3903	3409	0.873	3728	0.955	3584	0.918
21	C1-2.5-50-234-40-3(50)	3313	2860	0.863	3090	0.933	2975	0.898
22	C1-2.5-50-234-30-3(50)	2702	2285	0.846	2458	0.910	2371	0.878
23	C1-2.5-50-234-40-3(100)	3158	2860	0.906	3090	0.978	2975	0.942
24	C1-2.5-50-234-30-3(100)	2565	2285	0.891	2458	0.958	2371	0.925
25	C1-2.5-50-450-50-3(50)	4719	3957	0.839	4245	0.900	4101	0.869
26	C1-2.5-50-350-50-3(50)	4359	3717	0.853	4005	0.919	3861	0.886
27	C1-2.5-50-450-50-3(100)	4463	3957	0.887	4245	0.951	4101	0.919
28	C1-2.5-50-350-50-3(100)	4155	3717	0.895	4005	0.964	3861	0.929
	Mean			0.897		0.975		0.938
	SD			0.047		0.054		0.051
	COV			0.052		0.056		0.055

Table 2: Comparison of obtained ultimate load capacities (N_u) with predicted values by EC4 (2004) ($N_{pl,Rd}$) and proposed equations of Baig et al. (2006) (P_u) and Bahrami et al. (2013) (N_B)

5. CONCLUSIONS

This study has widely investigated the concrete-filled steel composite (CFSC) stub columns with steel stiffeners using the finite element software LUSAS. The existing experimental test results were used to compare with the results of the nonlinear analyses to verify the modelling. It was clearly demonstrated that the proposed finite element modelling was reasonably accurate to predict the behaviour of the columns herein. Novel steel stiffeners were used in the columns. The columns were extensively developed incorporating different special arrangements, number, spacing, and widths of the steel stiffeners with various steel thicknesses, concrete compressive strengths, and steel yield stresses. Effects of the variables on the behaviour of the columns were also examined. It was shown that using C1, C2, and C3 steel stiffeners increases the ultimate load capacity and ductility of the columns. Increasing the number or width of the steel stiffeners or steel thickness improves the ulti-

mate load capacity and ductility. Reducing the steel stiffeners spacing enhances the ultimate load capacity and ductility. The hierarchy of different arrangements of the steel stiffeners with same steel thickness and same number and spacing of the steel stiffeners from the ultimate load capacity and ductility views is C1, C3, and C2. As the concrete compressive strength increases the ultimate load capacity improves. Furthermore, the ultimate load capacity is increased if the steel yield stress is enhanced. In addition, the failure modes of the columns were recognised as concrete crushing of the columns about their mid-height where the local buckling of the steel wall was induced. The concrete infill prevented the inward buckling of the steel wall. Meanwhile, the obtained ultimate load capacities of the columns from the nonlinear analyses were compared with the predicted values by EC4 (2004) and the equations proposed by Baig et al. (2006) and Bahrami et al. (2013) which uncovered that EC4 (2004) predicts the ultimate load capacity of the columns more conservatively than the proposed Equations (7) and (8).

References

Bahrami, A., Wan Badaruzzaman, W.H. and Osman, S.A. (2011). Nonlinear analysis of concrete-filled steel composite columns subjected to axial loading. Structural Engineering and Mechanics - An International Journal 39(3): 383-398.

Bahrami, A., Wan Badaruzzaman, W.H. and Osman, S.A. (2013). Behaviour of stiffened concrete-filled steel composite (CFSC) stub columns. Latin American Journal of Solids and Structures 10: 409-439.

Baig, M.N., Jiansheng, F. and Jianguo, N. (2006). Strength of concrete filled steel tubular columns. Tsinghua Science and Technology 11(6): 657-666.

Dabaon, M., El-Khoriby, S., El-Boghdadi, M. and Hassanein, M.F. (2009). Confinement effect of stiffened and unstiffened concrete-filled stainless steel tubular stub columns. Journal of Constructional Steel Research 65: 1846-1854.

Ellobody, E. (2007). Nonlinear behavior of concrete-filled stainless steel stiffened slender tube columns. Thin-Walled Structures 45: 259-273.

Ellobody, E. and Young, B. (2006a). Design and behaviour of concrete-filled cold-formed stainless steel tube columns. Engineering Structures 28: 716-728.

Ellobody, E. and Young, B. (2006b). Nonlinear analysis of concrete-filled steel SHS and RHS columns. Thin-Walled Structures 44: 919–930.

Ellobody, E., Young, B. and Lam, D. (2006). Behaviour of normal and high strength concrete-filled compact steel tube circular stub columns. Journal of Constructional Steel Research 62(7): 706-715.

Eurocode 4, BS EN 1994-1-1, (2004). Design of composite steel and concrete structures- Part 1-1: General rules and rules for buildings, London: British Standard Institution.

Finite Element Analysis Ltd. (2006). LUSAS, User's Manual, Version 14, Surrey, UK.

Giakoumelis, G. and Lam, D. (2004). Axial capacity of circular concrete-filled tube columns. Journal of Constructional Steel Research 60(7): 1049-1068.

Han, L.H. and Yang, Y.F. (2003). Analysis of thin-walled steel RHS columns filled with concrete under long-term sustained loads. Thin-Walled Structures 41: 849–870.

Hu, H.T., Huang, C.S. and Chen Z.L. (2005). Finite element analysis of CFT columns subjected to an axial compressive force and bending moment in combination. Journal of Constructional Steel Research 61: 1692–1712.

Hu, H.T., Huang, C.S., Wu, M.H. and Wu, Y.M. (2003). Nonlinear analysis of axially loaded concrete-filled tube columns with confinement effect. Journal of Structural Engineering ASCE 129(10): 1322–1329.

Hu, H.T. and Schnobrich, W.C. (1989). Constitutive modeling of concrete by using nonassociated plasticity. Journal of Materials in Civil Engineering 1(4): 199–216.

Liew, J.Y.R. and Xiong, D.X., (2009). Effect of preload on the axial capacity of concrete-filled composite columns. Journal of Constructional Steel Research 65: 709-722.

Lin, M.L. and Tsai, K.C. (2001). Behaviour of double-skinned composite steel tubular columns subjected to combined axial and flexural loads. Proceedings of the First International Conference on the Steel & Composite Structures, Pusan, Korea, 1145-1152.

Mander, J.B., Priestley, M.J.N. and Park, R. (1988). Theoretical stress–strain model for confined concrete. Journal of Structural Engineering ASCE 114(8): 1804–1826.

Muciaccia, G., Giussani, F., Rosati, G. and Mola, F. (2011). Response of self-compacting concrete filled tubes under eccentric compression. Journal of Constructional Steel Research 67: 904-916.

Mursi, M. and Uy, B. (2003). Strength of concrete filled steel box columns incorporating interaction buckling. Journal of Structural Engineering ASCE 129(5): 626–639.

Petrus, C., Hamid, H.A., Ibrahim, A. and Parke, G. (2010). Experimental behaviour of concrete filled thin walled steel tubes with tab stiffeners. Journal of Constructional Steel Research 66: 915-922.

Richart, F.E., Brandzaeg, A. and Brown, R.L. (1928). A study of the failure of concrete under combined compressive stresses, Bull. 185. Champaign, IL, USA: University of Illinois Engineering Experimental Station.

Saenz, L.P. (1964). Discussion of 'Equation for the stress–strain curve of concrete' by Desayi, P. and Krishnan, S., Journal of American Concrete Institute 61: 1229–1235.

Tao, Z., Han, L.H. and Wang, Z.B (2005). Experimental behaviour of stiffened concrete-filled thin-walled hollow steel structural (HSS) stub columns. Journal of Constructional Steel Research 61: 962-983.

Tokgoz, S. and Dundar, C. (2010). Experimental study on steel tubular columns in-filled with plain and steel fibre reinforced concrete. Thin-Walled Structures 48: 414-422.

Tomii, M. (1991). Ductile and strong columns composed of steel tube infilled concrete and longitudinal steel bars, Special volume, Proceedings of the Third International Conference on Steel–Concrete Composite Structures, Fukuoka, Japan: Association of Steel-Concrete Structures.

Wang, Y.C. (1999). Tests on slender composite columns. Journal of Constructional Steel Research 49: 25–41.

Yang, Y.F. and Han, L.H. (2011). Behaviour of concrete filled steel tubular (CFST) stub columns under eccentric partial compression. Thin-Walled Structures 49: 379-395.

Zhao, X.L. and Grzebieta, R. (2002). Strength and ductility of concrete filled double skin (SHS inner and SHS outer) tubes. Thin-Walled Structures 40: 199–213.